Suppl. Figures

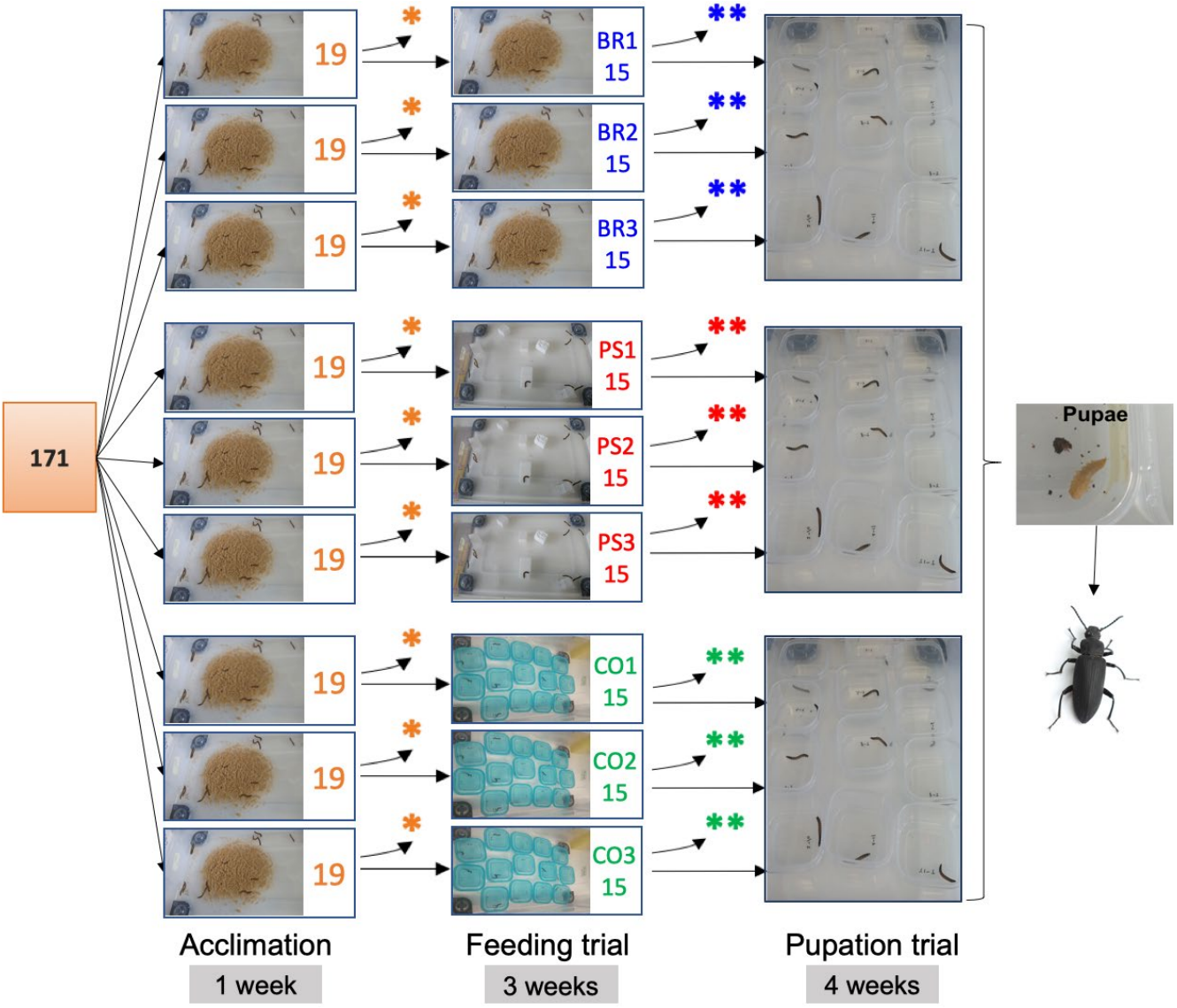

Figure S1 | Experimental layout of the superworm polystyrene diet experiment. In total, 171 worms were kept in nine containers during the acclimatization period of one week and fed with bran and carrots. At the start of the feeding trial the larvae were divided into three groups, each with three replicates (containers), which were labelled according to the food source: i) The bran group (**BR1, 2, 3**) was feed solely with bran, ii) the polystyrene group (**PS1, 2, 3**) had solely PS as food source and iii) the control group (**CO1, 2, 3**) received no food supply. Feeding for the BR and PS group occurred once a week. All three treatments were accompanied by misting the lid of the container with water to prevent the worms from dehydrating. Asterisks indicate the processing of larvae for microbiome analysis: * post acclimation period, 4 worms were randomly selected and removed from each container, one worm from each container was randomly selected for microbiome sequencing; ** post-feeding trial analysis, 1 worm from each container was randomly selected for microbiome sequencing.

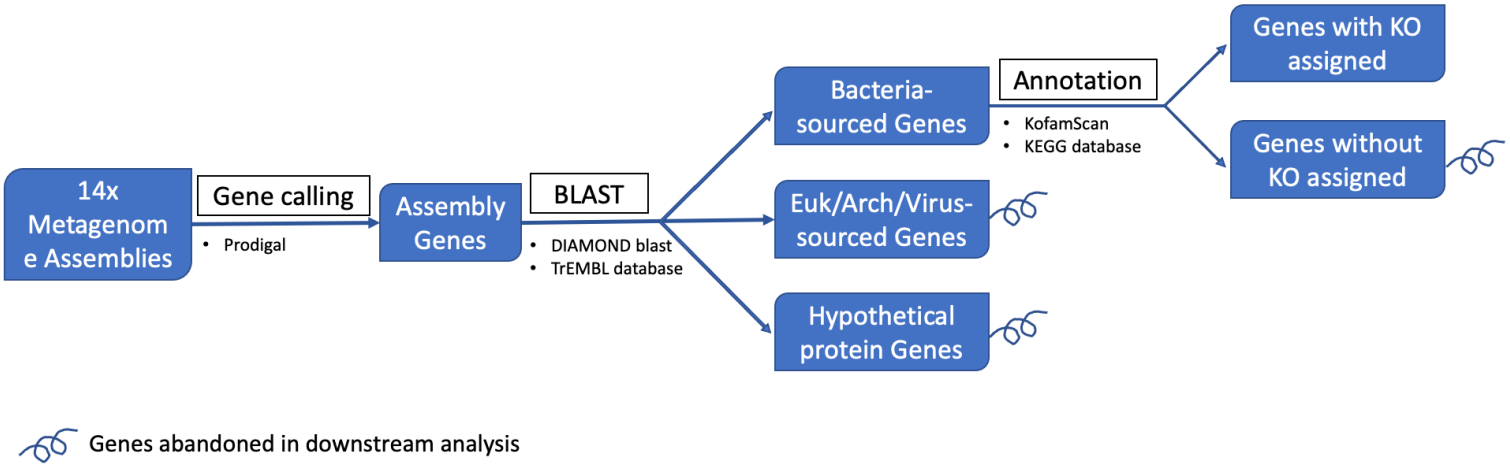

Figure S2 | Annotation of bacterial genes. Genes with a bacterial top blast hit were selected and annotated by KOfamScan for gene profiling analysis, while eukaryotic/ archaeal/ viral genes and genes without blast hits were excluded from the downstream analysis. “Hypothetical protein genes” are genes that did not have a blast hit.

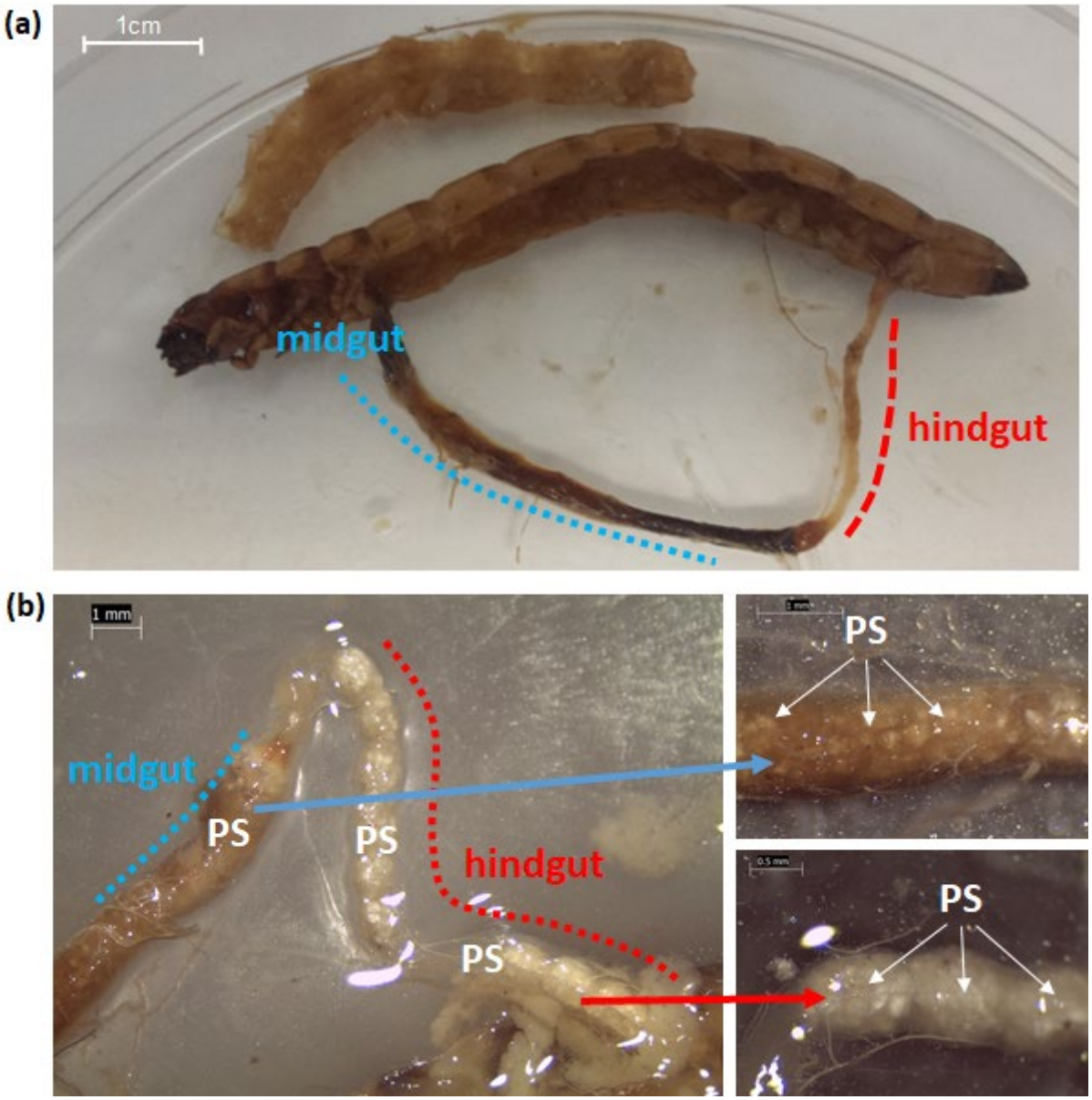

Figure S3 | Superworm anatomy and gut content. (a) Dissection of a superworm (*Zophobas morio*). Midgut and hindgut are highlighted. The removed ventral section is shown above the larvae. (b) Sections of mid- and hindgut tightly packed with polystyrene (PS) particles. Arrows pointing to higher magnification images of the PS packed midgut (upper image) and hindgut (lower image).

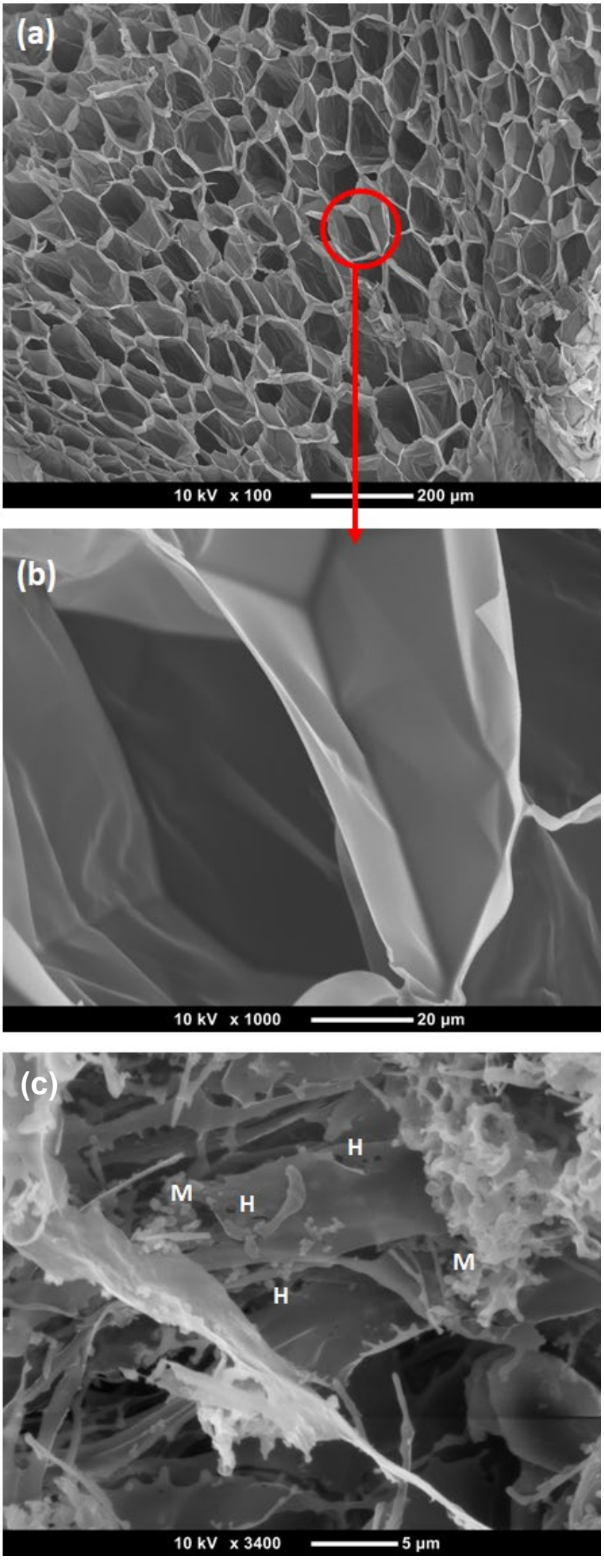

Figure S4 | Scanning electron pictures of polystyrene particles. (**a**) Scanning electron microscopy (SEM) image of the extruded polystyrene (styrofoam) as supplied by the manufacturer. (**b**) A higher magnification of the same particle (position in (a) is indicated by a red circle) showing the clean and intact PS foam structure. (**c**) Polystyrene particle recovered from the gut of a superworm in the PS group. Note the rugged structure of the PS, several holes (H), and microbial cells (M).

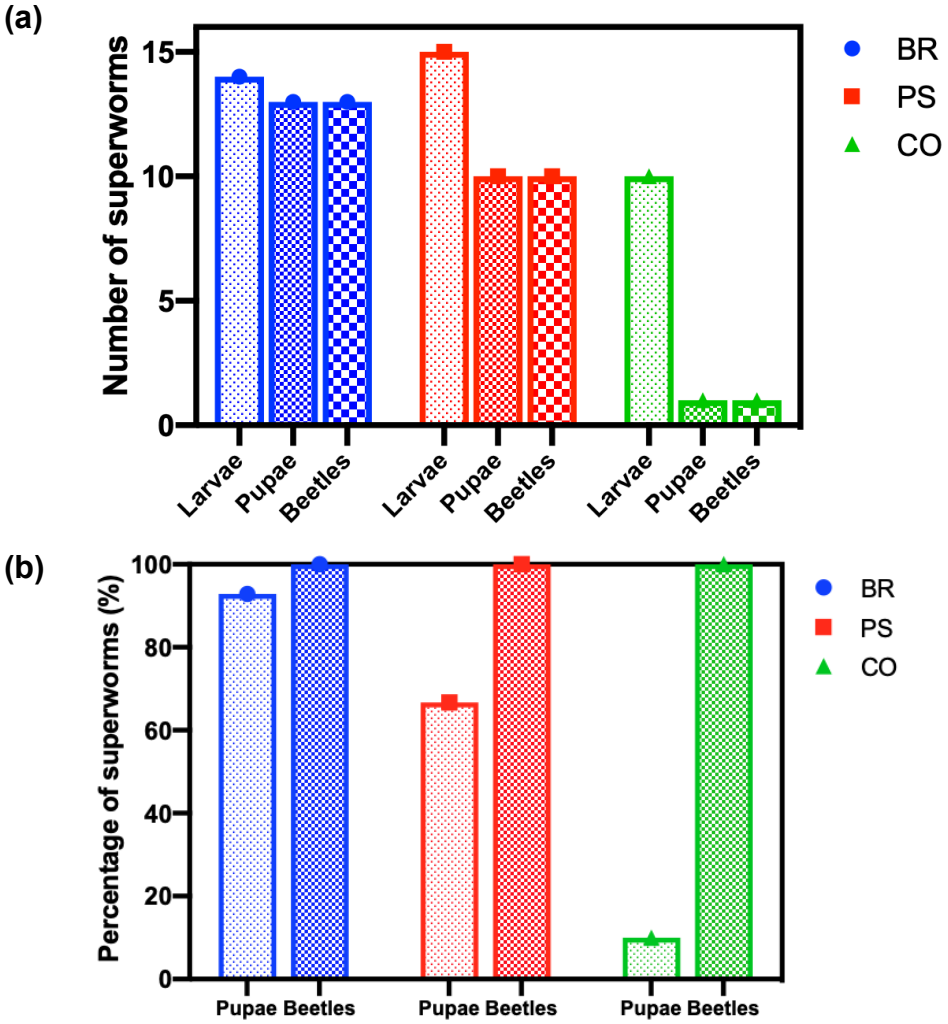

Figure S5 | Superworm pupation experiment. Numbers **(a)** and percentages **(b)** of superworms (Larvae) entering the pupae phase (Pupae) and emerging as live imago (Beetles) post transformation, are provided for all three feeding trials. Note that in (b) the percentage of pupae has been calculated by setting the number of larvae in each experiment to 100%, and the percentage of beetles has been calculated by setting the number of pupae in each experiment to 100%. Abbreviations: BR = bran group; PS = polystyrene group; CO = starvation control group.

(a)

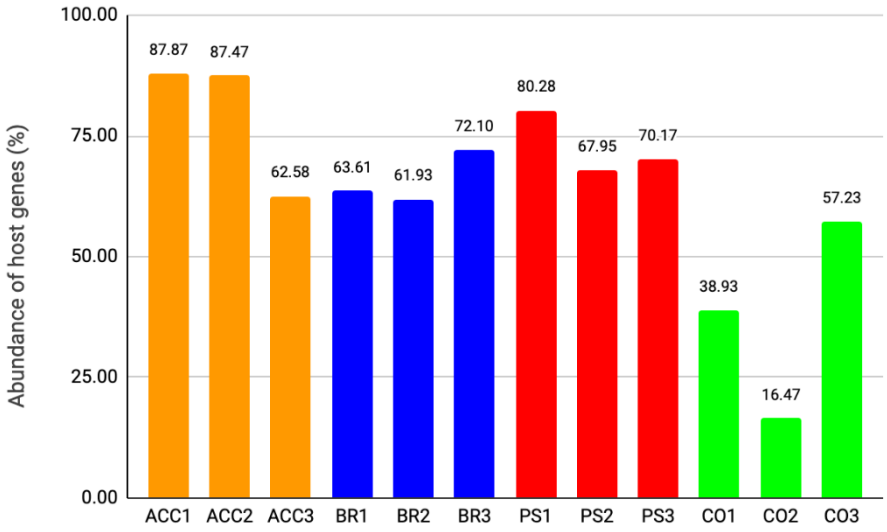
Abundance of host genes (%)
100.00
75.00
50.00
25.00
0.00
87.87
87.47
62.58
63.61
61.93
72.10
80.28
67.95
70.17
38.93
16.47
57.23
ACC1
ACC2
ACC3
BR1
BR2
BR3
PS1
PS2
PS3
CO1
CO2
CO3

(b) BR1

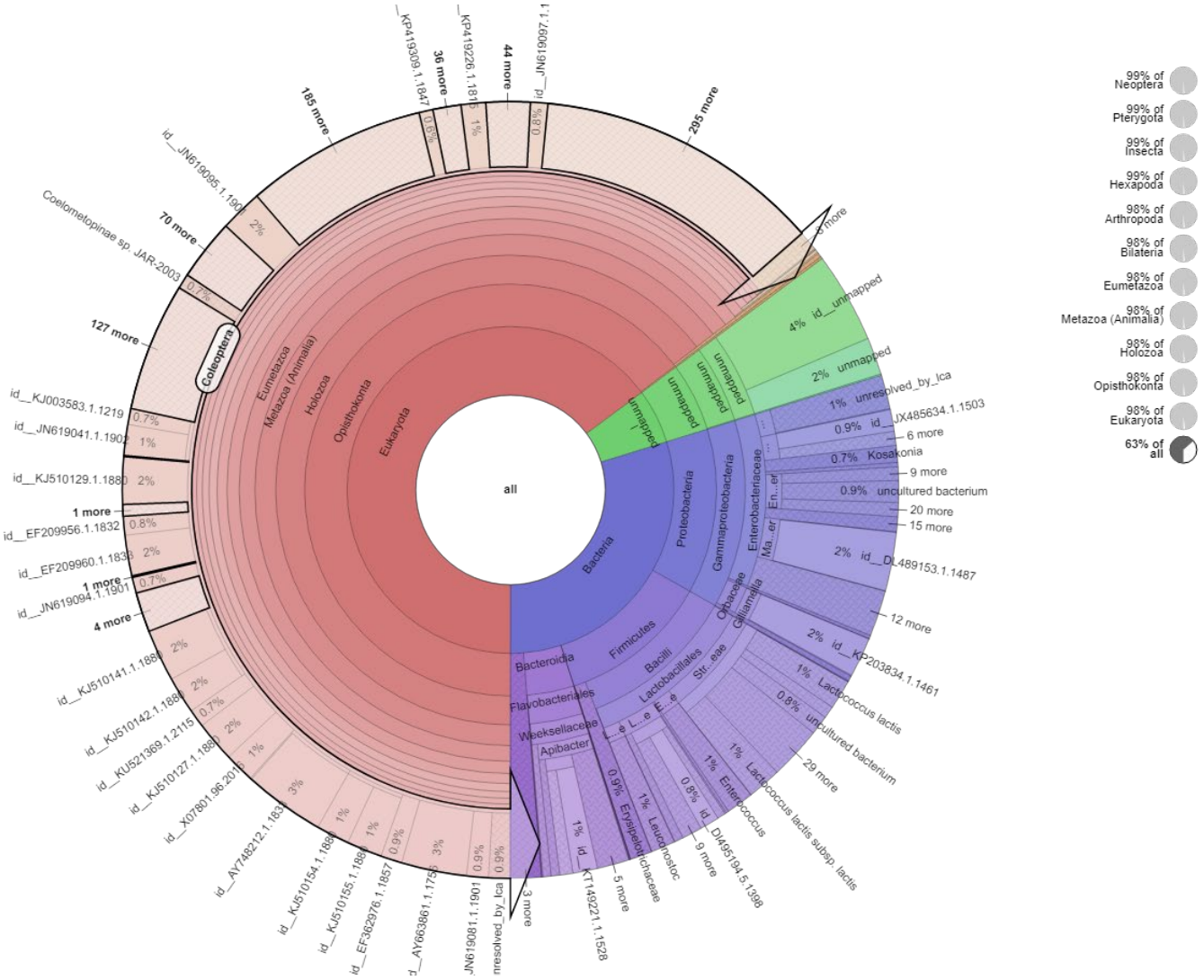
all
Bacteria
Eukaryota
Opisthokonta
Holozoa
Metazoa (Animalia)
Eumetazoa
Arthropoda
Hexapoda
Insecta
Pterygota
Neoptera
Proteobacteria
Gammaproteobacteria
Firmicutes
Bacilli
Bacteroidia
Coleoptera
Coelomeiopinae sp. JAR-2003
unmapped
unresolved_by_lca
uncultured bacterium
Kosakonia
Lactococcus lactis
Lactococcus lactis subsp. lactis
Enterococcus
Leuconostoc
Erysipelotrichaceae
Weeksellaceae
Apibacter
Flavobacteriales
Lactobacillales
Enterobacteriaceae
Obscuribacterales
Gillamaella
295 more
185 more
127 more
70 more
44 more
36 more
99% of Neoptera
99% of Pterygota
99% of Insecta
99% of Hexapoda
98% of Arthropoda
98% of Bilateria
98% of Eumetazoa
98% of Metazoa (Animalia)
98% of Holozoa
98% of Opisthokonta
98% of Eukaryota
63% of all

(c) PS1

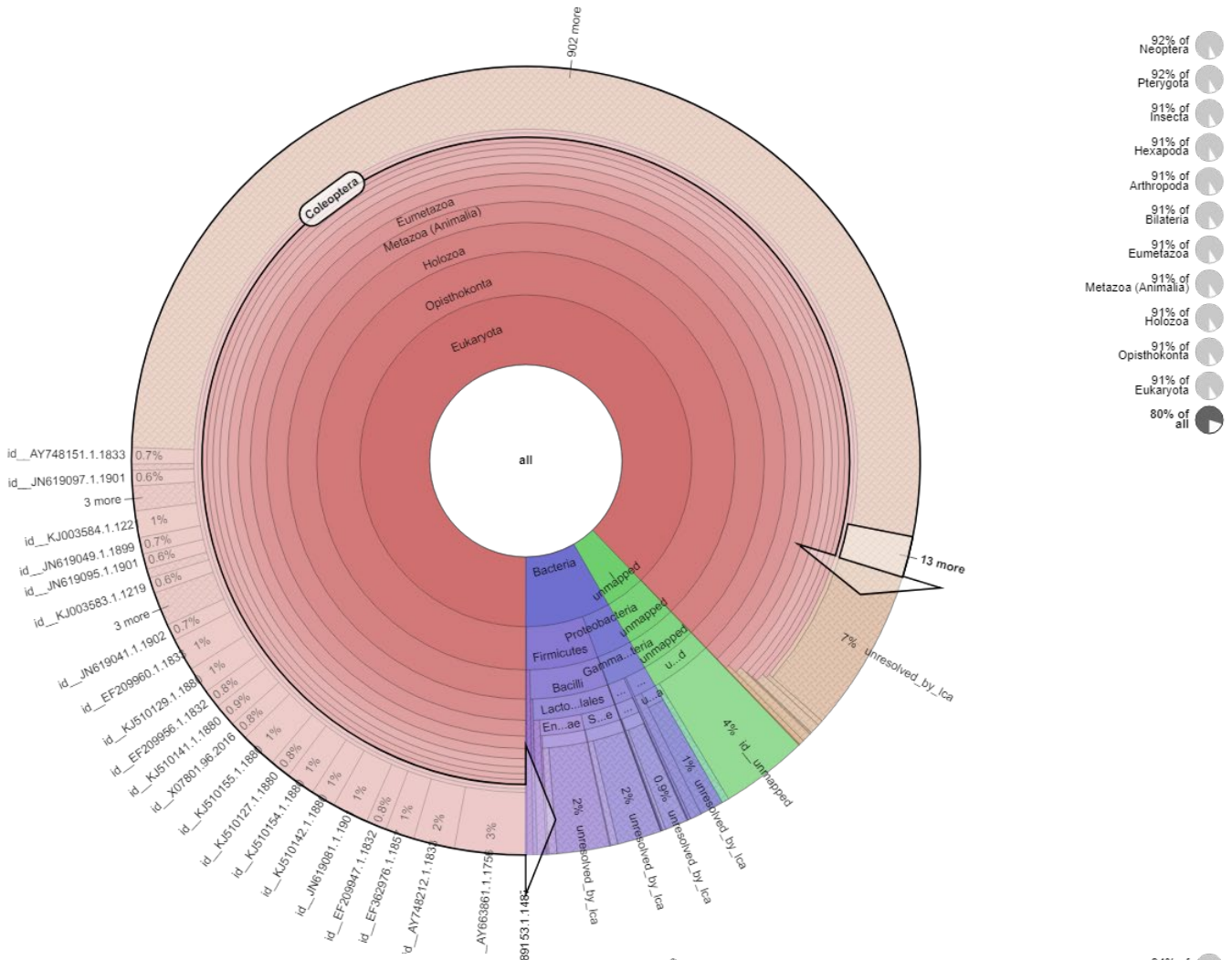
902 more
Coleoptera
Eumetazoa
Metazoa (Animalia)
Holozoa
Opisthokonta
Eukaryota
all
Bacteria
unmapped
Proteobacteria
Firmicutes
Bacilli
Lacto...lales
En...ae
S...e
13 more
7% unresolved_by_lca
4% id__unmapped
2% unresolved_by_lca
0.9% unresolved_by_lca
1% unresolved_by_lca
2% unresolved_by_lca
id__AY748151.1.1833 0.7%
id__JN619097.1.1901 0.6%
3 more
id__KJ003584.1.122 1%
id__JN619049.1.1899 0.7%
id__JN619095.1.1901 0.6%
id__KJ003583.1.1219 0.6%
3 more
id__JN619041.1.1902 0.7%
id__EF209960.1.1834 1%
id__KJ510129.1.188 1%
id__KJ510142.1.1832 0.8%
id__EF209956.1.1832 0.9%
id__KJ510141.1.1880 0.8%
id__X07801.96.2016 0.8%
id__KJ510155.1.1880 1%
id__KJ510127.1.1880 0.8%
id__KJ510154.1.1880 1%
id__JN619081.1.190 1%
id__EF209947.1.1832 0.8%
id__EF362976.1.185 1%
id__AY748212.1.1832 2%
id__AY663861.1.1756 3%
id__DL489153.1.1487
92% of Neoptera
92% of Pterygota
91% of Insecta
91% of Hexapoda
91% of Arthropoda
91% of Bilateria
91% of Eumetazoa
91% of Metazoa (Animalia)
91% of Holozoa
91% of Opisthokonta
91% of Eukaryota
80% of all

(d) CO1

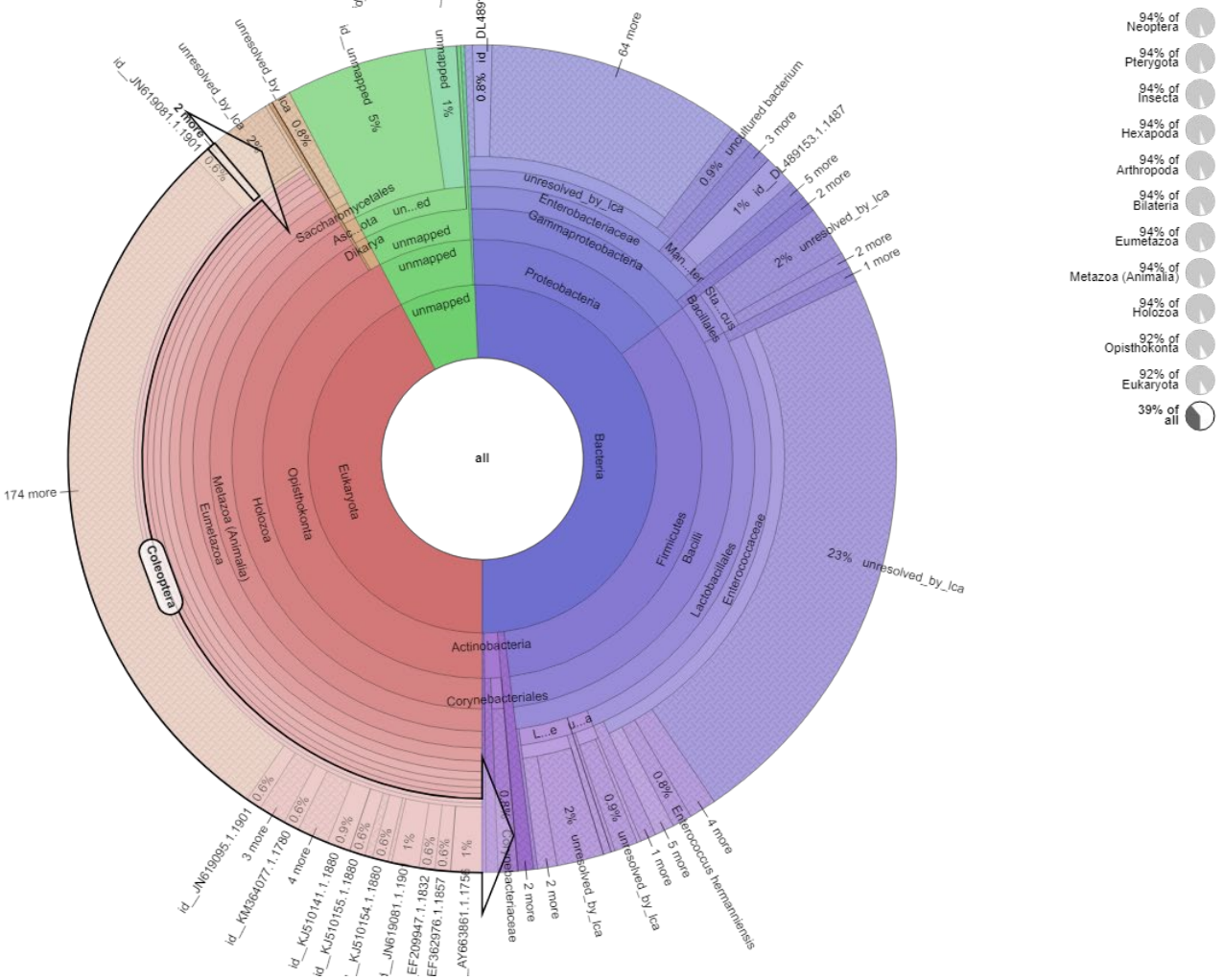
64 more
id__DL489153.1.1487
0.8%
unmapped
1%
id__unmapped 5%
unresolved_by_lca 0.8%
unresolved_by_lca 2%
id__JN619081.1.1901 0.6%
3 more
unresolved_by_lca
Enterobacteriaceae
Gammaproteobacteria
Proteobacteria
Bacteria
Firmicutes
Bacilli
Lactobacillales
Enterococcaceae
23% unresolved_by_lca
Actinobacteria
Corynebacteriales
Corynebacteriaceae
2% unresolved_by_lca
0.9% unresolved_by_lca
0.8% Enterococcus hermanniensis
4 more
5 more
1 more
2 more
2 more
1 more
0.9% uncultured bacterium
3 more
1% id__DL489153.1.1487
5 more
2 more
2% unresolved_by_lca
2 more
1 more
174 more
Coleoptera
Eumetazoa
Metazoa (Animalia)
Holozoa
Opisthokonta
Eukaryota
all
id__JN619095.1.1901 0.6%
3 more
id__KM364077.1.1780 0.6%
4 more
id__KJ510141.1.1880 0.9%
id__KJ510155.1.1880 0.6%
id__KJ510154.1.1880 0.6%
id__JN619081.1.190 1%
id__EF209947.1.1832 0.6%
id__EF362976.1.1857 0.6%
id__AY663861.1.1756 1%
94% of Neoptera
94% of Pterygota
94% of Insecta
94% of Hexapoda
94% of Arthropoda
94% of Bilateria
94% of Eumetazoa
94% of Metazoa (Animalia)
94% of Holozoa
92% of Opisthokonta
92% of Eukaryota
39% of all

Figure S6 | Estimated proportion of superworm host genes in metagenomes. (a) Host gene proportions were calculated by dividing the number of 18S rRNA reads assigned to 'p__Arthropoda' by the number of total rRNA (16S and 18S) reads based on read assignments by graftM using the custom package "4.40.2013_08_greengenes_97_OTUs_with_euks.gpkg". Abbreviations: ACC: Acclimation period (pre feeding trials); BR: Bran group; PS: PS group; CO: control starvation group. **(b, c, d)** Krona plots of detailed taxonomic profiles including eukaryotic hits of the metagenomes bran 1 (BR1) in b), polystyrene 1 (PS1) in c), and the starvation control 1 (CO1) in d). Taxonomic assignments are based on CommunityM profiles (https://github.com/dparks1134/CommunityM), and the order Coleoptera (beetles) is highlighted in the Krona plots with a black outline.

Please note the **low proportion of host genes in the control group (CO 1-3)** in (a). We can exclude the possibility that this low proportion of host genes was caused by an increase in 18S genes from other eukaryotes, such as fungi, since nearly all eukaryotic genes were assigned to the insect host in CO (d). What we found is a strong shift in the ratio of host to microbial genes in the starvation group, compared to all other groups (b, c, d). Our hypothesis is that the lower proportion of host genes in the starvation control group are caused by gut dysbiosis and a subsequent thinning of the gut lumen. We used the entire mid- and hindgut for DNA extraction, which resulted in ~60-80% host reads (a), except for the control group, which contained between 15% and 57% host genes. We noted that the guts from the starvation group superworms seemed thinner and more fragile, and therefore we hypothesize that dysbiosis has caused a thinning of the gut lumen, which resulted in lower numbers of inset gut cells and hence a lower percentage of host DNA in the starvation samples. Indeed, mouse models have shown that dysbiosis causes thinning and disorganization of the epithelial layer (Chen et al. 2019).

Chen, Song, Yuhua Zheng, Yiqing Zhou, Weizhong Guo, Qin Tang, Guangli Rong, Weiwei Hu, Jianbang Tang, and Huanhuan Luo. 2019. "Gut Dysbiosis with Minimal Enteritis Induced by High Temperature and Humidity." *Scientific Reports* 9 (1): 18686. https://doi.org/10.1038/s41598-019-55337-x.

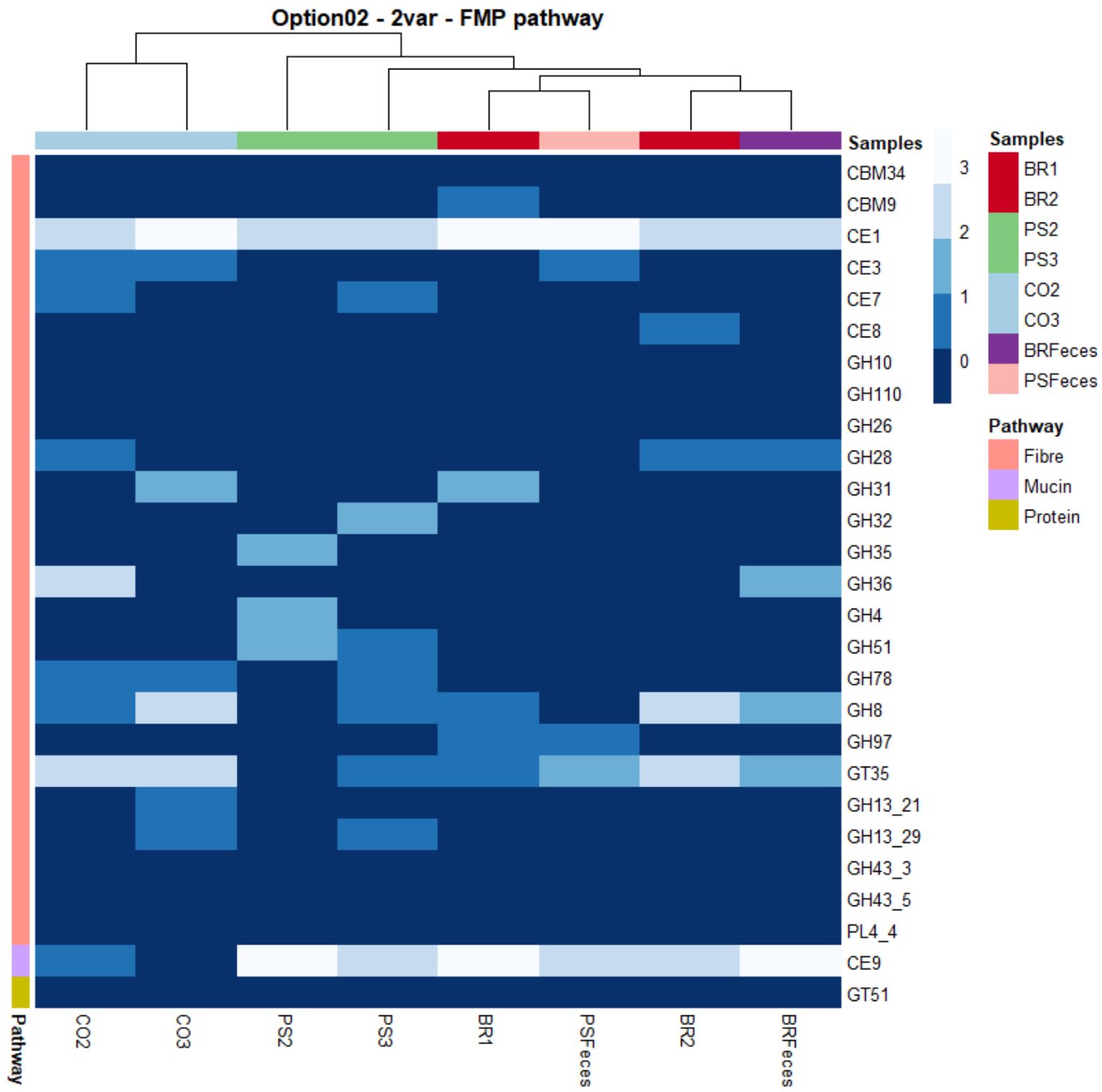

Figure S7 | Bacterial genes involved in fiber, mucus, and protein degradation, annotated against CAZy. The heatmap includes samples from the bran group (BR), the polystyrene group (PS), the starvation control group (CO), the polystyrene feces (PSF), and the bran feces (BRF). The y-axis is sorted by fiber, mucus, and protein degrading abilities.

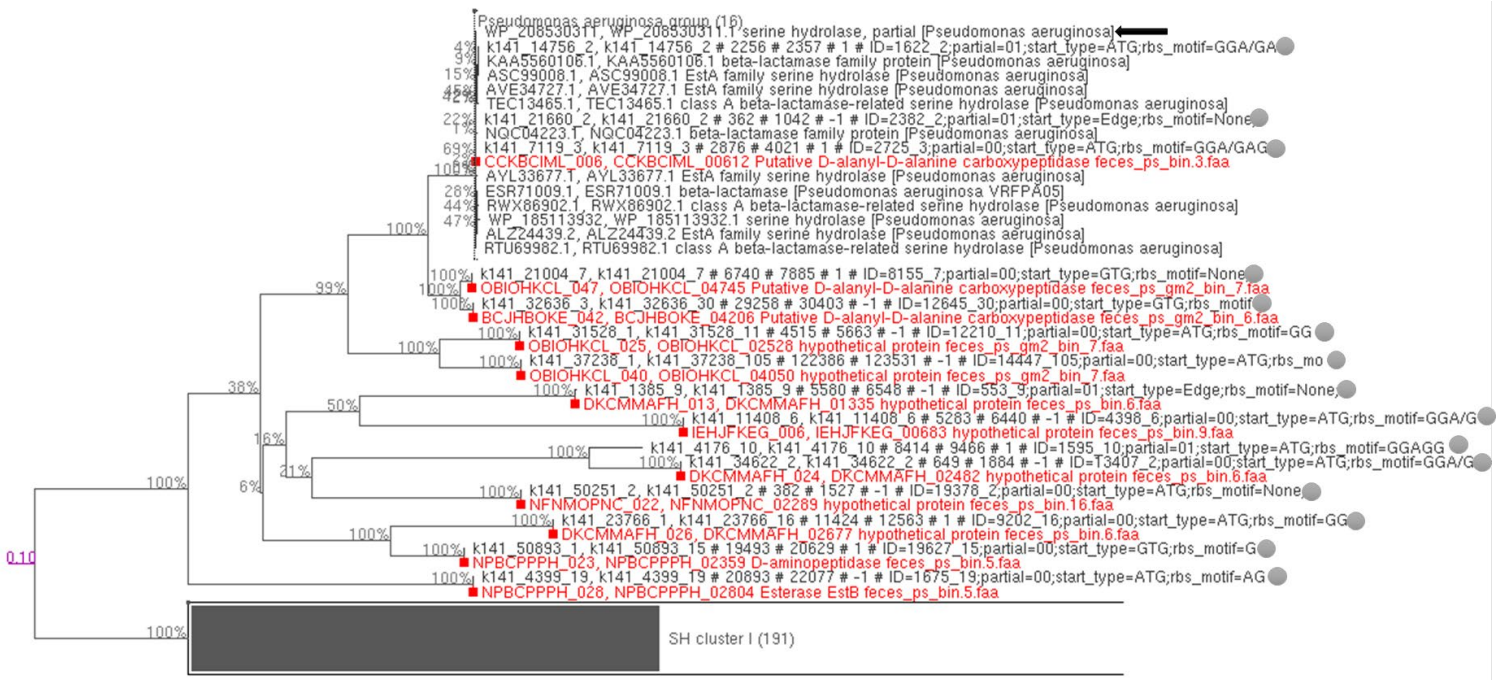

Figure S8 | Phylogenetic tree of serine hydrolase genes. Homologues of WP_208530311.1, the gene encoding serine hydrolase in *Pseudomonas aeruginosa* (black arrow), were retrieved from assemblies and MAGs by a blastp search with evalue <1e-5. The phylogenetic tree was inferred with IQ-TREE (LG+C10+F+G+PMSF model) from a 998-position alignment with true bootstrap support values (gray numbers at internal nodes) based on 100 trees inferred under the same model. The tree was rooted between the group containing the reference serine hydrolase sequence and the rest. Fifteen sequences from assemblies (gray dots) and twelve from MAGs (red font) of sample Feces-PS and PS1 were clustered with WP_208530311.1, suggesting they represent true homologues of serine hydrolase genes and could translate into a protein involved in the breakdown of polystyrene.

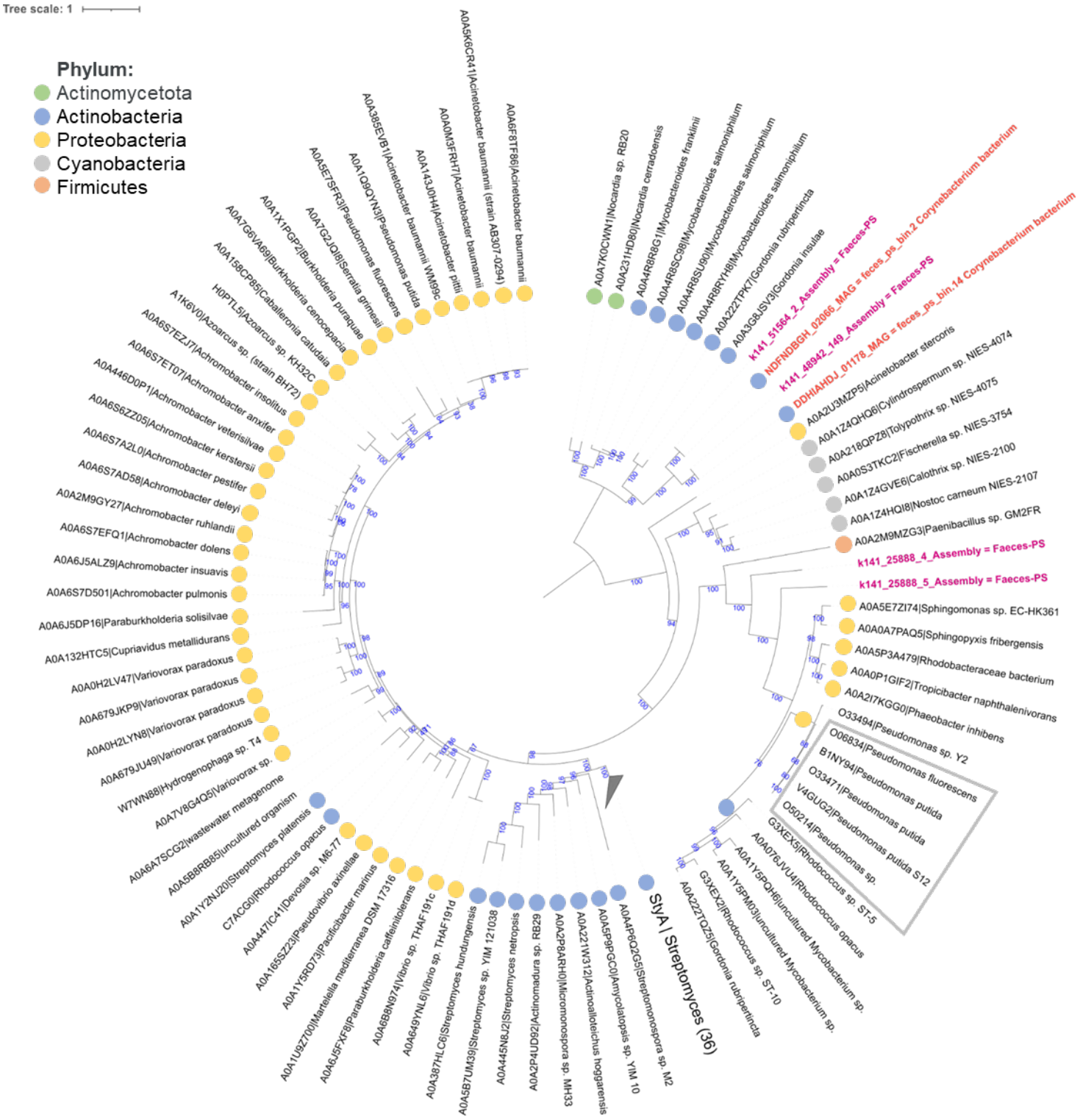

Figure S9 | Phylogenetic tree of styA gene homologues encoding styrene monooxygenase. The phylogenetic tree was inferred with IQ-TREE (LG+C10+F+G+PMSF model) from a 787-position alignment with ultrafast bootstrap support values (blue numbers at internal nodes) based on 1000 ultrafast trees under the same model. The tree was rooted on the group containing two StyA sequences from MAGs (red) and two StyA from Faeces-PS assembly (pink). The styA genes of the experimentally verified enzymes in *Pseudomonas fluorescens, Pseudomonas putida,* and *Pseudomonas sp.* are highlighted in a grey box.

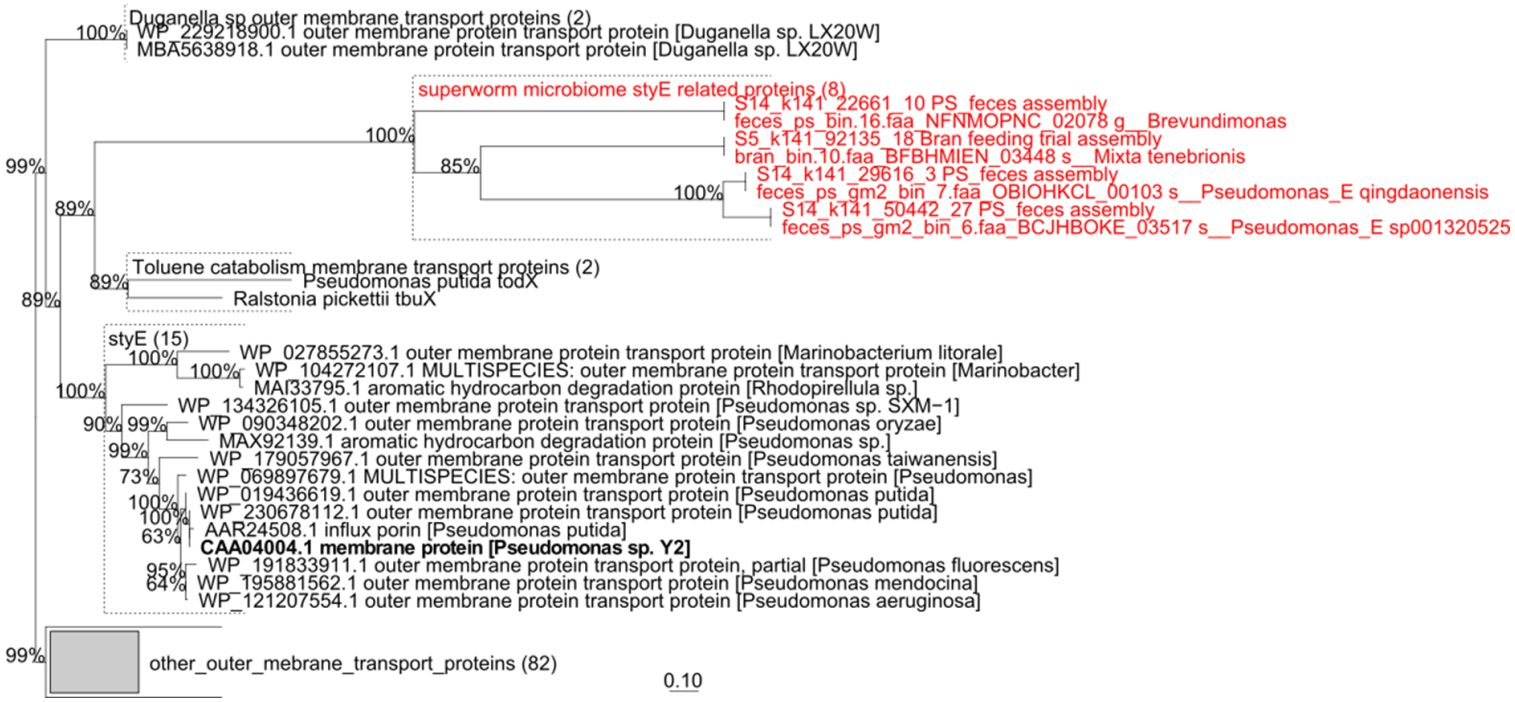

Figure S10 | Phylogenetic tree of styE gene homologues encoding an outer membrane protein involved in styrene transport. Homologues of the StyE encoding gene from Pseudomonas sp. Y2 (highlighted in bold) were retrieved from NCBI (blastp; 100 best hits), and were recovered from the superworm microbiome assemblies and MAGs (blastp, <e-10; highlighted in red). In addition, two genes, which represent membrane proteins involved in toluene catabolism, from the INTERPRO family "Outer membrane protein transport protein (OMPP1/FadL/TodX) IPR005017“, which includes styE, were added. The phylogenetic tree was inferred with IQ-TREE (LG+C10+F+G+PMSF model) with ultrafast bootstrap support values based on 100 ultrafast trees inferred under the same model.

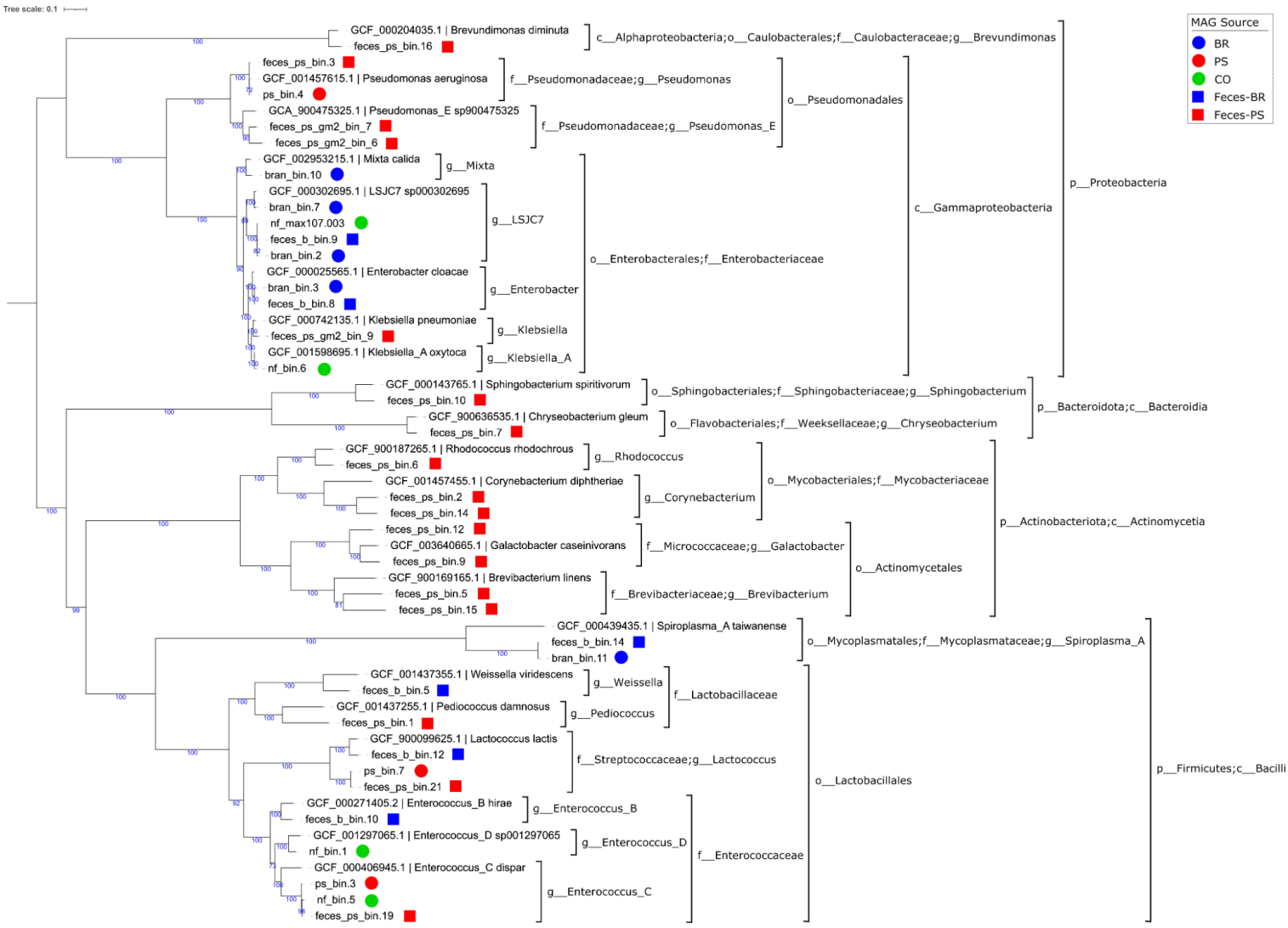

Fig. S11 | Phylogenetic tree of metagenome-assembled genomes (MAGs) recovered in this study. A multiple sequence alignment of 56 genomes (35 MAGs plus 21 GTDB species-representative genomes selected from the same genera as the MAGs) was created based on 120 marker genes using gtdb-tk. Starting trees were inferred with FastTree under the JTT+CAT model and used for IQ-TREE under the LG+C10+F+G+PMSF model. 100 bootstrap trees were calculated under the same IQ-TREE model, and bootstrap values above 70% are shown on the corresponding branches.